Thin Solid Films 517 (2008) 691–694

Contents lists available at ScienceDirect

Thin Solid Films

journal homepage: www.elsevier.com/locate/tsf

# Combinatorial study of the crystallinity boundary in the $HfO_2$–$TiO_2$–$Y_2O_3$ system using pulsed laser deposition library thin films

P.K. Schenck *, J.L. Klamo, N.D. Bassim, P.G. Burke, Y.B. Gerbig, M.L. Green

*Ceramics Division, National Institute of Standards and Technology, 100 Bureau Drive STOP 8520, Gaithersburg, Maryland 20899-8520, USA*

ARTICLE INFO

*Article history:*
Received 23 May 2008
Received in revised form 31 July 2008
Accepted 4 August 2008
Available online 14 August 2008

*Keywords:*
High-k dielectrics
Combinatorial
Thin films
Reflectometry
X-ray diffraction
Nanoindentation

ABSTRACT

$HfO_2$–$TiO_2$–$Y_2O_3$ is an interesting high-*k* dielectric system, with the potential for higher values of *k* than the end members. Combinatorial library films of this system enable the study of the role of composition on phase formation as well as optical and mechanical properties. A library film of this system deposited at 400 °C exhibited a boundary line evident visually as well as in characterization. Mapping X-ray analysis showed the line corresponds to a crystallinity boundary, separating an amorphous phase and a face-centered cubic crystalline phase of yttrium hafnium oxide. Mapping nanoindentation across the boundary also revealed a sharp change in mechanical properties. The combinatorial technique is a powerful tool for high-throughput materials science, and by realizing this particularly unique pulsed laser deposition library film, allows many interesting materials phenomena and properties to be measured.



## 1. Introduction

The development of combinatorial materials research [1,2] has allowed researchers to study wide ranges of materials by producing library films with varying compositional coverage. The combinatorial technique can be used for the optimization of film properties and the discovery of *unique* materials for use in thin film devices. *Combinatorial pulsed laser deposition (PLD)*, featuring nearly congruent vaporization of target materials, can be used to produce binary and ternary library films of complex stoichiometry with continuous composition spreads [3]. In this letter, we report the observation of the crystallinity boundary in the $HfO_2$–$TiO_2$–$Y_2O_3$ system in a combinatorial library film. The dielectric system discussed here utilizes three technologically-relevant materials that have been suggested for use in high-*k* applications [4–6].

## 2. Experimental procedures

The library films in this work were produced using a commercial combinatorial PLD tool (Pioneer 180-CCS, Neocera [7]). The PLD tool uses a multiple target carousel combined with an indexed rotating substrate holder/heater to produce library films. The production of ternary library films consists of depositing a sub-monolayer of target one at 0°, indexing the substrate to 120°, depositing a sub-monolayer from the second target, indexing the substrate to 240°, and depositing a sub-monolayer from the third target. This sequence is repeated until the desired thickness of the library film is obtained. The required recipe for this sequence is determined by first calibrating the deposition rates from the three targets under the conditions of chamber pressure, laser fluence, etc. used for the deposition of the library film. The calibration procedure consists of depositing the three single composition films and determining the deposition distribution. Since the films from the $HfO_2$, $TiO_2$, and $Y_2O_3$ targets are transparent in the visible-near infrared region (400 nm to 950 nm), high throughput spectroscopic reflectometry [8] is used to map the thickness distribution of the single component films. This procedure, described in detail elsewhere [9], produces a recipe of number of laser shots per target and number of times to repeat the cycle for the desired deposition thickness. This also allows us to predict the composition at each point on the library film. The conditions chosen for this library film, using a KrF excimer laser (248 nm) focused to a fluence of ~15 J/cm$^2$, were a deposition distance of 6.5 cm, substrate temperature of 400 °C, and oxygen background pressure of 13.3 Pa. The substrates were 76.2 mm diameter 100 silicon wafers. The recipe used for the $HfO_2$–$TiO_2$–$Y_2O_3$ library film consisted of 25 laser pulses for $HfO_2$, 36 laser pulses for $TiO_2$, and 47 for $Y_2O_3$, repeated 250 cycles to achieve a nominal 275 nm thick library film (as measured at the center). Fig. 1 shows the as-deposited $HfO_2$–$TiO_2$–$Y_2O_3$ library film. The clearly visible line between the $TiO_2$-rich region and the rest of the film prompted detailed characterization of the film by optical, X-ray, and nanoindentation studies. The originally intended composition-varying library sample exhibited a unique phenomenon of interest in terms of metrology, as the particularly accessed region of processing space included at least two phases.

The $HfO_2$–$TiO_2$–$Y_2O_3$ library film was characterized with X-ray diffraction (XRD) measurements (D8 DISCOVER, Bruker AXS, equipped

* Corresponding author. Tel.: +1 301 975 5758; fax: +1 301 975 5334.
*E-mail address:* pkschenck@nist.gov (P.K. Schenck).

0040-6090/$ – see front matter © 2008 Elsevier B.V. All rights reserved.
doi:10.1016/j.tsf.2008.08.001

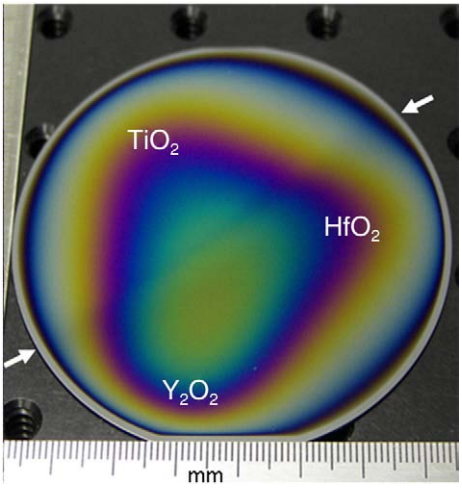


**Fig. 1.** Digital photograph of the $HfO_2$–$TiO_2$–$Y_2O_3$ library film showing a clear boundary across the film (arrowed) separating the $TiO_2$ rich region from the $HfO_2$–$Y_2O_3$ region. The image was obtained at an angle to avoid a direct reflection, thus foreshortening the image.

with a crossed-wire area detector). The sample stage has 2 translation axes for sample placement such that the library film could be moved to collect from different locations (i.e., compositions). XRD data were collected for each point on the library sample at ambient temperature using Cu-Kα radiation for 100 s. The scattered intensity of a particular point on the library film was measured over a range of $22.5° < 2\theta < 57.5°$, with the detector held fixed at $2\theta = 40°$, and with X-rays incident to the sample at $\omega = 20°$. The resulting data were integrated over the range of $-62° < \chi < -115°$ (where $\chi$ is the second axis of the 2-D detector, the azimuthal angle defining the direction of the diffracted beams on the diffraction cone) to provide a single graph of integrated intensity versus $2\theta$. After single peaks are identified, raw data is fit to a Gaussian using a least squares algorithm. The center value of the Gaussian fit corresponds to a particular $2\theta$, and allows particular peak d-spacings to be extracted and tabulated.

The nanomechanical properties of the central portion of the $HfO_2$–$TiO_2$–$Y_2O_3$ library film were mapped using a nanoindenter (TriboIndenter®, Hysitron) with a three-sided pyramidal Berkovich indenter tip. A thicker library film, nominally 585 nm in the center but otherwise grown under identical conditions, was fabricated to insure reliable measurements of the thin film properties and exclude any major influence of the silicon substrate. In the indentation tests, a maximum load of 500 μN was applied with a continuous loading rate of 50 μN/s. The maximum load was held for 5 s and afterward withdrawn with an unloading rate of 50 μm/s. Hardness and reduced elastic modulus of the thin film were determined using the method of Oliver and Pharr [10]. From the reduced elastic *modulus* $E_r$, the elastic modulus E of a thin film can be calculated with $1/E_r = 1/(E - \nu^2)$ whereby $\nu$ is the Poisson's ratio (which is the ratio of the transverse strain to the axial strain). For comparison purposes, nanoindentation tests were performed for separately grown $TiO_2$, $Y_2O_3$ and $HfO_2$ thin films under the same conditions as described for the library film.

## 3. Results

### 3.1. Optical properties

A high throughput mapping spectroscopic reflectometer was used to measure the reflectivity and estimate the thickness of the library film by assuming an average value for the index of refraction $(n - ik)$ based on the indices of the three materials (with $k = 0$) [11,12]. The film was modeled as a bilayer using an effective medium model [13] for the surface layer, to accommodate the faceted surface structure discussed below in Section 3.2. The model assumed that the surface layer had an index of refraction that was proportional to the index of refraction of the lower layer of the film. The total thickness of the film, including this surface layer, is shown in Fig. 2A. The map of the effective surface layer thickness, shown in Fig. 2B, clearly shows the visible line of Fig. 1. Fig. 2B shows that the line is due to a change in the surface layer across the line, as the lower right region of the sample has a thicker surface layer consisting of crystalline facets. This line, or boundary, is also evident in a map of the effective surface layer index of refraction (not shown). Additional analysis of the reflectivity data, allowing the index of refraction to vary over the film, did not significantly change the thickness of the surface layer.

### 3.2. Microstructure

The results of the X-ray mapping of the central region of the film, combined with composition information of the $HfO_2$–$TiO_2$–$Y_2O_3$ library film, are shown in Fig. 3. The ternary format of Fig. 3 is used to illustrate the predicted compositional coverage of the library film. The small black points indicate the predicted composition over the 76.2 mm wafer, and the larger points indicate the sub-area of X-ray mapping. The d-spacing derived from the peak at nominally $2\theta = 34.5°$ (with a detector resolution corresponding to ±0.015°), corresponding to the 200 diffraction peak of a face-centered cubic phase of yttrium hafnium oxide, exhibits a monotonic change with composition. The d-spacing of the yttrium hafnium oxide 200 peak increases with increasing $Y_2O_3$ content, as has been shown previously [14,15]. Additionally, as more $TiO_2$ is incorporated into

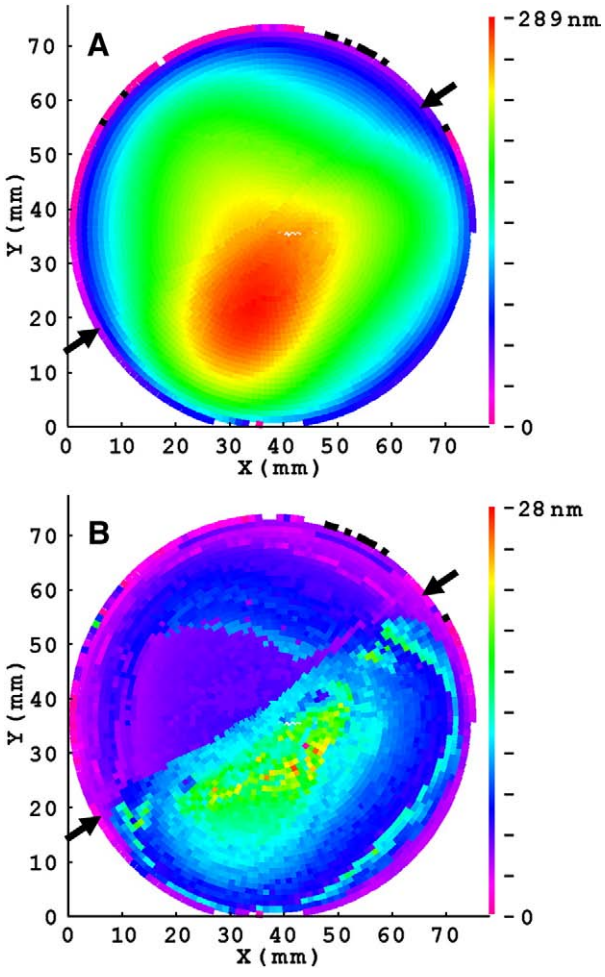


**Fig. 2.** Thickness map (A) and surface layer (B) of the $HfO_2$–$TiO_2$–$Y_2O_3$ library film showing a clear line across the film (arrowed as in Fig. 1).

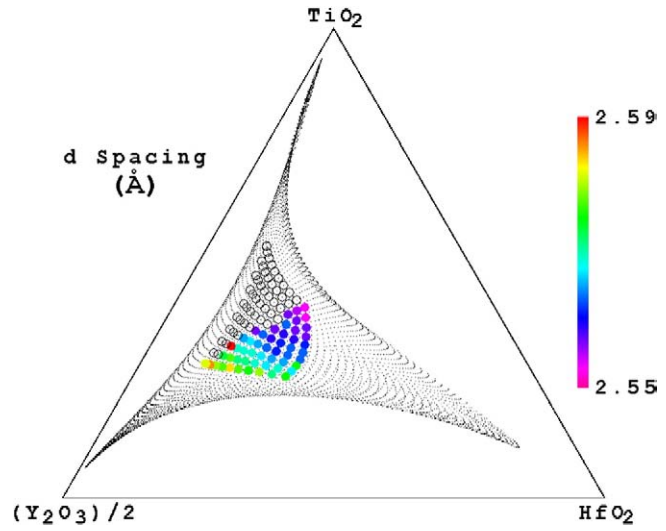


**Fig. 3.** Ternary diagram showing the predicted compositional coverage (small points) of the $HfO_2$–$TiO_2$–$Y_2O_3$ library film and the derived d-spacing (large points, in Å, 10 Å = 1 nm) of the 200 peak of yttrium hafnium oxide.

the film, the d-spacing decreases. The open data points in Fig. 3 indicate regions where there was no diffraction and thus are assigned to be amorphous. Based on our single-composition calibrations, corroborated with previous work [4], it is known that $TiO_2$ is amorphous at lower growth temperatures, such as the 400 °C growth here. Hence, at some critical incorporation of $TiO_2$, the film can no longer sustain the formation of the yttrium hafnium oxide phase. The line visible by optical analysis therefore corresponds to the border of the crystalline to amorphous region of the library film. Scanning electron microscope (SEM) images of the amorphous and crystalline regions are shown in Fig. 4. With increasing $TiO_2$ composition in the library film, the microstructure changes from dense, faceted grains to an amorphous structure. Also, the crystalline grain size shown in Fig. 4B corroborates well with the model for surface thickness in Fig. 2B. The faceted surface structure implied in the model is the result of the crystalline nature of this region.

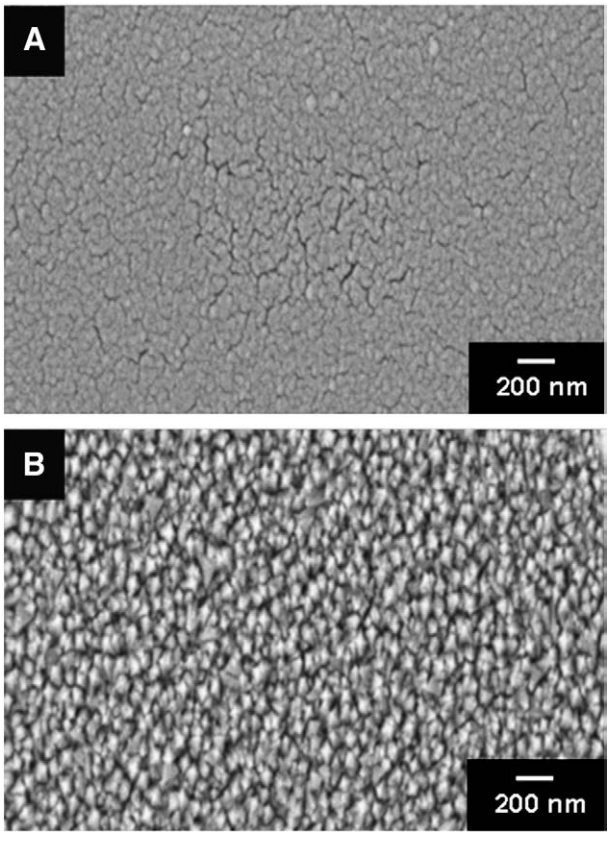


**Fig. 4.** SEM images of the amorphous (A) and crystalline (B) regions of the $HfO_2$–$TiO_2$–$Y_2O_3$ library film.

### 3.3. Nanomechanical properties

Fig. 5 shows the values for hardness and reduced elastic modulus determined over the library film in the region of the line. Here, the colored points specify the sub-area of nanoindentation mapping. The maps reveal two distinct regions of mechanical properties, separated by a relatively narrow transition region. For the amorphous region, hardness and modulus values range from 4.21 GPa to 3.69 GPa and 84 GPa to 110 GPa, whereas significantly lower values were measured for the crystalline region ($H$ = 1.44 GPa to 1.99 GPa, $E_r$ = 47 GPa to 62 GPa). The transition region marks the boundary between amorphous and crystalline microstructure in Fig. 3.

A comparison between the mechanical properties of the amorphous region of the library film and those measured on a $TiO_2$ thin film

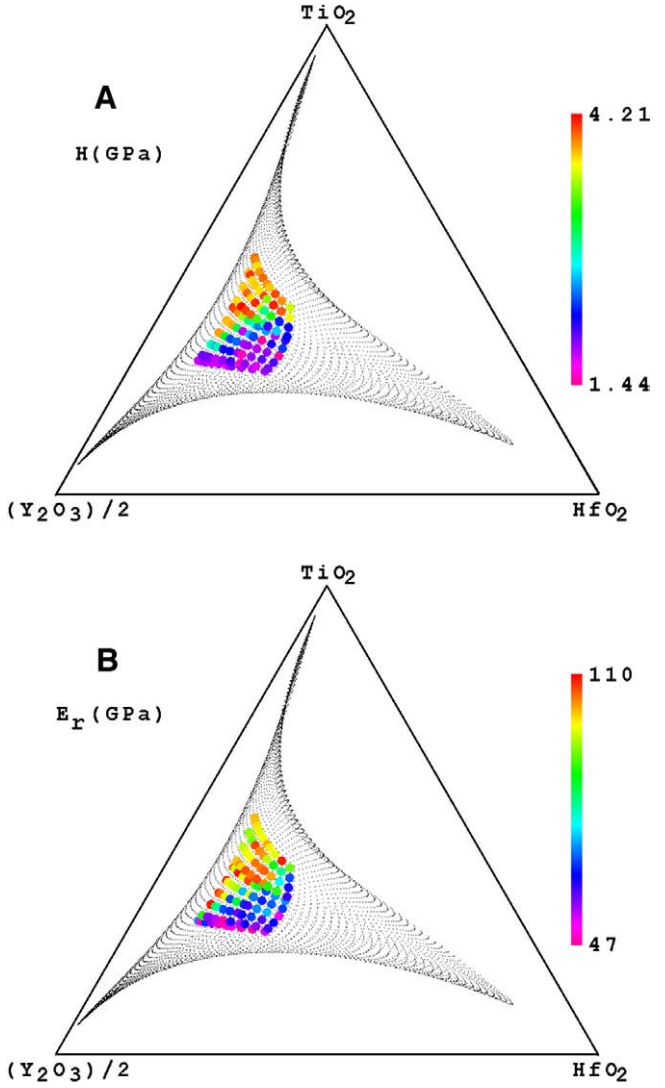


**Fig. 5.** Ternary diagram showing the predicted compositional coverage (small points) of the $HfO_2$–$TiO_2$–$Y_2O_3$ library film and (A) the hardness H (large points) (in GPa) and (B) the reduced elastic modulus $E_r$ (large points) (in GPa), both determined via nanoindentation technique.

showed similar results ($H$=4.1±0.17 GPa, $E_r$ = 116±8 GPa, where the error is the standard deviation of 20 indents). This indicates that $TiO_2$ dominates the mechanical behavior of the library film in this region. It should be noted that the data presented in this study for amorphous $TiO_2$ films are comparable to values reported for this type of thin film in the literature [16,17]. The drop in hardness and modulus when going from the amorphous region to the crystalline region can most likely be attributed to a stronger contribution of the $HfO_2$ and $Y_2O_3$ components in the crystalline region of the library film. Therefore, the library films resemble more of the mechanical properties of both of these components, which were determined to be $H$=2.87±0.11 GPa and $E_r$ = 55±4 GPa (for $HfO_2$) and $H$=2.33±0.19 GPa and $E_r$ = 116±9 GPa (for $Y_2O_3$).

## 4. Conclusion

Combinatorial PLD is an excellent metrology tool for screening technologically relevant high-$k$ complex oxide systems. High throughput characterization of the library films including spectroscopic reflectometry, X-ray diffraction, and nanoindentation have been used to map the properties of the films as a function of composition. These techniques confirm the observation of an amorphous to crystalline boundary, in composition space, in the $HfO_2$–$TiO_2$–$Y_2O_3$ ternary system. The role of process parameters, such as substrate temperature, on the properties of these films is the subject of ongoing research.

## Acknowledgments

One of the authors, P.G.B., was supported in part by the National Science Foundation's Research Experience for Undergraduates (REU) program, Division of Materials Research.

## References

[1] J.J. Hanak, J. Mater. Sci. 5 (1970) 946.
[2] X.D. Xiang, X. Sun, G. Briceño, Y. Lou, K.-A. Wang, H. Chang, W.G. Wallace-Freedman, S.W. Chen, P.G. Schultz, Science 268 (1995) 1738.
[3] H.M. Christen, S.D. Silliman, K.S. Harshavardham, Rev. Sci. Instrum. 72 (2001) 2673.
[4] G.D. Wilk, R.M. Wallace, J.M. Anthony, J. Appl. Phys. 89 (2001) 5243.
[5] K. Kita, K. Kyuno, A. Toriumi, Appl. Phys. Lett. 86 (2005) 102906.
[6] M. Komatsu, R. Yasuhara, H. Takahashi, S. Toyoda, H. Kumigashira, M. Oshima, D. Kukuruznyak, T. Chikyow, Appl. Phys. Lett. 89 (2006) 172107.
[7] Certain commercial equipment, instruments, or materials are identified in this document. Such identification does not imply recommendation or endorsement by the National Institute of Standards and Technology, nor does it imply that the products identified are necessarily the best available for the purpose.
[8] P.K. Schenck, D.L. Kaiser, A.V. Davydov, Appl. Surf. Sci. 223 (2004) 200.
[9] N.D. Bassim, P.K. Schenck, M. Otani, H. Oguchi, Rev. Sci. Instrum. 78 (2007) 072203.
[10] W.C. Oliver, G.M. Pharr, J. Mater. Res. 7 (1992) 1564.
[11] E.D. Palik, Handbook of Optical Constants of Solids, Academic Press, Boston, 1991.
[12] G.E. Jellison, L.A. Boatner, J.D. Budai, B.S. Jeong, D.P. Norton, J. Appl. Phys. 93 (2003) 9537.
[13] H.G. Tompkin, W.A. McGahan, Spectroscopic Ellipsometry and Reflectometry A User's Guide, John Wiley and Sons, New York, 1999, p. 125.
[14] K. Kita, K. Kyuno, A. Toriumi, Appl. Phys. Lett. 86 (2005) 102906.
[15] D.W. Stacey, D.R. Wilder, J. Am. Ceram. Soc. 58 (1975) 285.
[16] H. Takikawa, T. Matsui, T. Sakakibara, A. Bendavid, P.J. Martin, Thin Solid Films 348 (1999) 145.
[17] T. Modes, B. Scheffel, C. Metzner, O. Zywitzki, E. Reinhold, Surf. Coat. Technol. 200 (2005) 306.